

Helium permeation through mixed matrix membranes based on polyimides and silicalite-1

Marie Fryčová^{1,2}, Petr Sysel², Pavel Hrabánek¹, Milan Kočířík¹, Libor Brabec¹, Arlette Zikánová¹, Bohumil Bernauer², Pavel Čapek², Vladimír Hejtmánek³

¹J. Heyrovský Institute of Physical Chemistry of ASCR, v.v.i., Dolejškova 3, 182 23 Prague 8-Libeň, Czech Republic

²Institute of Chemical Technology, Technická 3, 166 28 Prague 6-Dejvice, Czech Republic

³Institute of Chemical Process Fundamentals of ASCR, v.v.i., Rozvojová 135, 16502 Prague 6, Czech Republic

Corresponding author:

Milan Kočířík

Dept. of Structure and Dynamics in Catalysis

J. Heyrovský Institute of Physical Chemistry of ASCR, v.v.i.

CR 182 23 Prague

E-Mail: milan.kocirik@jh-inst.cas.cz

Abstract

Mixed matrix membranes based on modified polyimides and silicalite-1 were prepared and studied. The novel preparation approach consists in improvement of the interfacial adhesion by employment of the coupling agent 3-aminopropyltriethoxysilane in such a way which leads to forming of chemical bonds between polyimide and silicalite-1. Firstly polyimide chains were endcapped by this agent which subsequently enabled their reaction with groups naturally present on silicalite-1 surface. Membranes with silicalite-1 content up to 60 wt. % were prepared and characterized by SEM, light microscopy and permeation of gases, prevailingly of He. The accessibility of silicalite-1 pores prior to embedding and after embedding into polymeric matrices was studied by an iodine indicator technique. The permeability of membranes for gases was measured using a semi-open permeation apparatus with a small volume. Helium permeability depended on filler content and increased monotonously with the increasing content of filler. There were, however, significant deviations of the permeability dependences on filler content from shapes predicted by Bruggeman's model. The qualitative explanation of the data disagreement with the model was proposed based on a stratification of mixed matrix membranes found by SEM.

Mixed matrix membranes, polyimide, zeolite, silicalite-1, gas permeability, helium.

1. Introduction

Gas separation by selective permeation through polymer membranes is one of the fastest growing branches of separation technology. The permeability of pure polymeric membranes for gases has its upper bound which can be overcome by formation of mixed matrix membranes containing as the other constituent particles of a microporous sorbent

[1]. The feasibility of preparation procedures to manufacture polyimide based membranes with enhanced permeability for gases was examined in the present work using silicalite-1 crystals as the microporous constituent. The effect of silicalite-1 content on membrane permeability of self-standing composite membranes was studied using non-stationary measurement of gas permeation carried out in a quasi-steady state regime. The prevailing test penetrant used was helium.

2. Experimental

Chemicals

4,4'-(hexafluoroisopropylidene)diphthalic anhydride (6FDA), Chriskev;
Pyromellitic dianhydride (PMDA), Aldrich;
5,5'-oxybis-1,3-isobenzofurandione (ODPA), Chriskev;
4,4'-(1,4-phenylenediisopropylidene)bisaniline (BIS P), Mitsui;
4,4'-oxydianiline, (ODA), Aldrich;
3-aminopropyltriethoxysilane (APTES), ABCR;
N,N-dimethylformamide (DMF), Aldrich;
TOSIL, Czech industrial product produced by Tonaso Neštěmice
Tetrapropylammonium bromide, Fluka;
Sodium bicarbonate, Solvay;

Silicalite-1 preparation

The silicalite-1 crystals were grown by reacting silica sol (Tosil), tetrapropylammonium bromide and sodium bicarbonate. The reaction gel was heat-treated in Teflon-lined stainless steel autoclave at autogenous pressure without stirring. The size of the crystals was controlled by selecting the proper duration of crystallization which was in the range between 8 and 24 h. Temperature of the synthesis was 180°C. After slow cooling of the autoclave, the crystals were filtered, washed and dried as described in [2]. The template tetrapropylammonium cation was removed in a single stage calcination process under the flow of an air stream of 600 ml.min⁻¹. The following heating program was applied to the shallow bed of crystals: heating up at the rate of 0.5°C.min⁻¹ until reaching 550°C, maintaining at 550°C for 12 h and cooling at the rate of 2°C.min⁻¹ to the laboratory temperature.

Polymer precursor preparation

All glassware was dried in an oven at 120°C for 3 h before use and the syntheses were carried out under an inert atmosphere to exclude the effect of air humidity. The polyamic acids (PAAs) with controlled molecular mass M_n were terminated by 3-aminopropyltriethoxysilane (APTES) and prepared in a 250 ml two-necked flask equipped with a magnetic stirrer and a nitrogen inlet/outlet. A typical example of the synthesis of the terminated PAA of this type (with $M_n = 10\,000\text{ g}\cdot\text{mol}^{-1}$) is as follows: 5.9257 g (0.01910 mol) ODPA was dissolved in 30 ml of DMF and 0.4543 g (0.00205 mol) of the terminating agent (APTES) was added (the weighing dish + funnel was rinsed with 15 ml DMF) to the reaction mixture and allowed to react with ODPA for 2 h. 3.6583 g (0.01827 mol) ODA (15 ml DMF used for rinsing) was then added and the reaction was

2

allowed to proceed at room temperature for 24 h. The 15 wt. % solution of PAA obtained in this way was rather viscous and thus it was diluted by addition of another portion of the same solvent to resulting concentration of 10 wt. %. These diluted PAA solutions were used as the precursors of PIs.

Membrane preparation

Mixed matrix membranes PI – Silicalite-1 were prepared by adding the zeolite crystals to the solution of the precursor under stirring. The content of the calcined zeolite in the resulting composites ranged as a rule from 0 to 50 wt. %. Occasionally, the upper limit of zeolite content was even 60 wt. %. The preparation of suspension under stirring proceeded for at least 1 h.

The prepared dispersion was cast on Teflon support. After evaporating the solvent, the films were gradually thermally imidized at 100°C/1h, 150°C/1h, 200°C/2h and 230°C/1h. The PI sheets were easily removed from the Teflon and used for characterization and/or further treatment. The thickness of the films increased with content of the filler.

Iodine indicator technique

The iodine indicator technique (IIT) is an original technique developed in our laboratory which allows among others a quick check of accessibility of pores of zeolites. In relation to composites it was reported for the first time to characterize accessibility of silicalite-1 crystals in polyimides in Ref. [3]. Iodine molecule is represented by a cylinder of 0.40 nm × 0.66 nm [4], [5]. This size fits well in the oxygen windows of MFI type structure (straight channels 0.56 nm × 0.53 nm and sinusoidal channels 0.51 nm × 0.55 nm). Fine iodine particles representing the source of iodine vapour were placed at the beginning of the colouring experiment into a minicell together with a sample. All the observations were made at 25°C in ambient air. The colouring of crystals proceeded rapidly in case when no strongly sorbed molecules were present in silicalite-1 channels. Pre-adsorbed species, however, may considerably retard the colouring kinetics [6]. All the colouring experiments in the present study were performed in the vapour phase by contacting the iodine particles with the sample. The colouring was monitored using the light microscopy (PERAVAL, Interphako, Carl Zeiss, Jena) coupled with a digital camera (Nikon Coolpix 95). The sorption kinetics was monitored by taking coloured photographs at different contact time. These photographs were used to check accessibility of the pores after template removal. To run colouring experiments with PI-Silicalite-1 composites, circular discs of the diameter of about 5 mm were cut from the foil. The experiments then started by contacting the iodine particles with either side of the foil. Each circular disc was cut from the same foil as the corresponding membrane for permeation test.

Permeation measurements

Three non-stationary permeation apparatuses of similar construction were built to measure permeation of gases through the membranes [7]. A typical arrangement of a permeation apparatus constructed to measure very low molar flows of gases which was used in this work is shown in Fig. 1.

3

The apparatus (Fig. 1) was equipped with two pressure gauges. The gauge with lower excess pressure range made possible to start depressurization runs with maximum starting pressure excess Δp_0 of 150 kPa. The other one extended this region to 2.5 MPa. The apparatuses differed from each other in size of the total measuring volume V_{Σ} which was represented for measuring of low permeation flows by the total volume of the tubing (i.e. $V_{t1}+V_{t3}+V_{t4}$). This was the only way to minimize the magnitude of the measuring volume which was a necessary condition to measure very low permeability. Any depressurization run was started after pressurization of the volume $V_{t1}+V_{t4}$ by opening the valve S_3 . All the measurements were carried on at room temperature (i.e. 25°C).

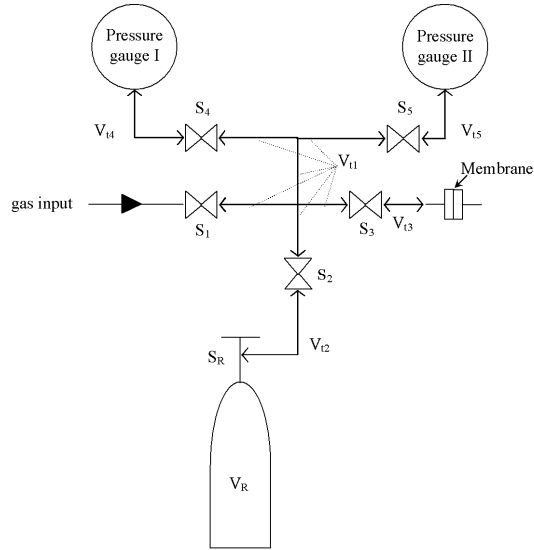


Fig. 1: Scheme of the permeation apparatus. $V_{t1} \dots V_{t5}$ are volumes of the respective tubing sections, V_R is cylinder volume and $S_1 \dots S_R$ are stopcocks.

The basis for treatment of permeation runs is formed by Eq (2) which represents the mass balance equation for the permeation apparatus combined with the constitutive equation (1).

$$j = P \frac{\Delta p}{\delta} = P \frac{p - p_a}{\delta} \quad (1)$$

$$-\frac{d\Delta p}{dt} = \frac{PRTQ}{V_{\Sigma} \delta} \Delta p = \alpha \Delta p \quad (2)$$

In these equations P is the membrane permeability [$\text{mol.m}^{-1}.\text{s}^{-1}.\text{Pa}^{-1}$], δ is membrane thickness, p is the actual pressure in the apparatus and p_a represents the ambient pressure, further on j is the flow density [$\text{mol.m}^{-2}.\text{s}^{-1}$] of the penetrant through the membrane in the direction of the membrane normal pointing out of the apparatus and Q denotes the membrane cross-sectional area.

It should be noted that the validity of Eq (2) is a consequence of the assumption on the existence of so called quasi-stationary state. This assumption means that at any time instant there is established a steady-state concentration profile of the penetrant in the

membrane. The condition necessary for the existence of the quasi-stationary state in the membrane is the validity of the relation (3):

$$\frac{V_{\Sigma}}{RT} \gg Q\delta K_{\Sigma} \quad (3)$$

where K_{Σ} is the overall Henry's law constant for the penetrant in the composite membrane. The condition (3) was fulfilled for our apparatuses with He used as penetrant. Solution of Eq (2) subject to initial condition $\Delta p(0) = \Delta p_0$ can be written in the form of Eq (4), which is comfortable for evaluation of permeability P .

$$\ln\{\Delta p(t)/\Delta p_0\} = \ln\{\exp(-\alpha t)\} = -\alpha t \quad (4)$$

3. Results and discussion

Membrane constituents

Matrix

Polyimides modified by the coupling agent 3-aminopropyltriethoxysilane (APTES) used as the matrix of membranes are listed in Fig. 2.

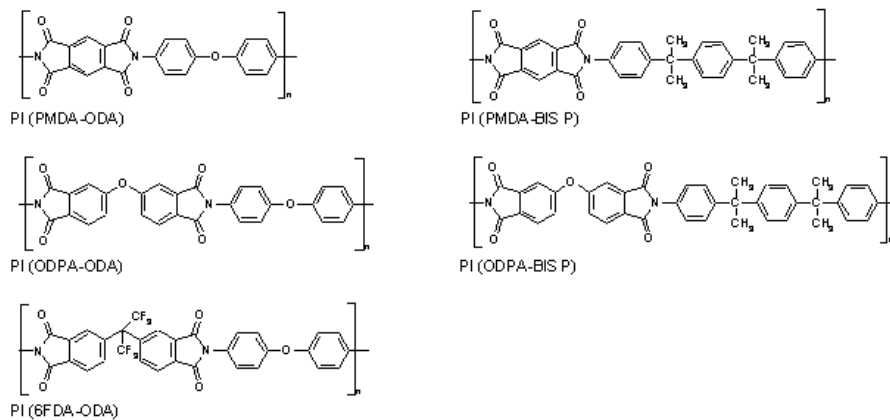
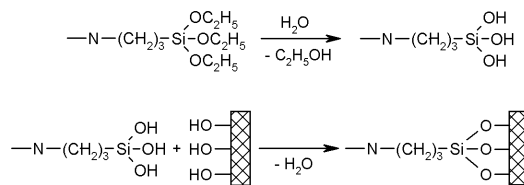


Fig. 2: The types of polyimides used as the matrix of membranes

Each of these APTES modified PIs was found to form a consistent membrane filled with silicalite-1 crystals, whereas without APTES only PI based on 6FDA and ODA formed mixed matrix membranes filled with silicalite-1. This corresponds with a presumption of a Si-O-Si group formation between the

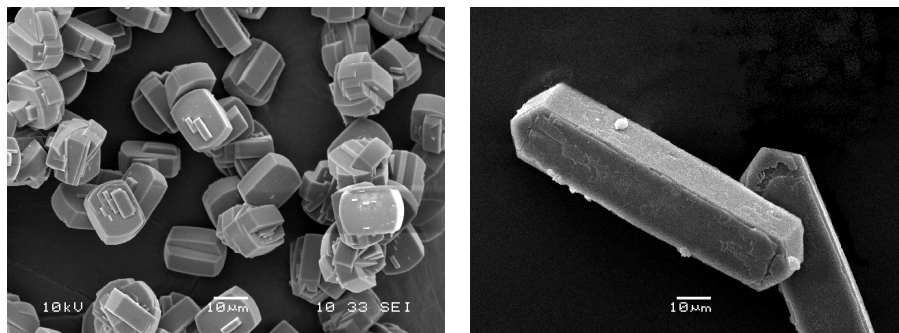


polymer matrix and the zeolite surface groups. The reaction between the end groups of the modified polyimides and the groups on the external zeolite surface may proceed at elevated temperatures during transformation of PAA into the final PI as shown in Fig. 3.

Fig. 3: Formation of chemical bonds between the end groups of the polymer and the groups on the surface of the zeolite.

Silicalite-1 crystals used as fillers

From the silicalite-1 samples prepared according to the procedure described above were selected as filling materials for the present study those with crystal size 20 μm and 100 μm. These silicalite-1 crystals were (i) coffin-shaped crystals of crystal length $L_c = 100 \mu\text{m}$ and (ii) boat-shaped crystals of crystal length $L_c = 20 \mu\text{m}$ as it is shown in Fig. 4.



silicalite-1-20 μm

silicalite-1-100 μm

Fig. 4: SEM photos of the silicalite-1 crystals that were used as fillers of membranes.

The Si/Al ratio of the prepared silicalite-1 crystals was found to fall into the range 350 to 360. Due to low Al content the silicalite-1 samples were sufficiently hydrophobic and for this reason all the manipulation with silicalite-1 crystals could be carried in the presence of atmospheric humidity. Thus, IIT could also be applied on air. The application of IIT showed a full accessibility of silicalite-1 channels selected for embedding in polymers. The result of IIT experiment was a colouring of initially colourless crystals to dark violet tint as exemplified by a light microscope image (Fig. 5).

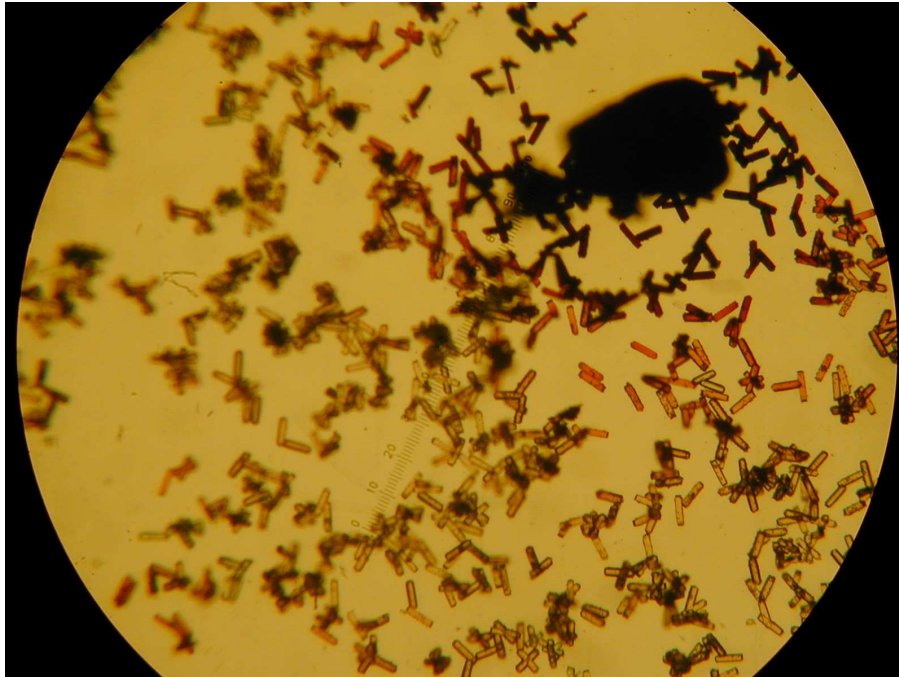


Fig. 5. Picture of colouring process of non-embedded crystals free of template taken a few seconds after their contact with an iodine particle (the big black corpuscle).

Preparation and characterization of membrane and its constituents

Polymer

In most cases, powder of the solid dianhydride is added to diamine solution. The reverse order (i.e. solid diamine addition to dianhydride solution) was used to preparation of PAAs with controlled M_n . The amount of APTES was calculated for a way to prepare the PAA with controlled $M_n = 10\,000\text{ g.mol}^{-1}$ and molecules endcapped by APTES. There is a relationship between M_n and the amount of the end groups. In general, the higher amount of the end groups the shorter molecular chains and lower M_n . It means that one has to choose optimal amount of APTES to obtain polymer with sufficiently high M_n and amount of the reactive end groups.

All PAAs were prepared as 15 wt. % solution in DMF and subsequently diluted to 10 wt. % solution in DMF. The concentration of PAA controls the thickness of membrane. The higher concentration of PAA results in the higher viscosity of solution and the higher thickness of the final membrane. On the other hand too low concentration of PAAs causes formation of defects in the films.

The above described procedure was used to prepare all PAAs terminated by APTES with the theoretical $M_n = 10\,000\text{ g.mol}^{-1}$. These were based on monomer combinations

7

PMDA-ODA, ODPA-ODA, PMDA-BIS P, ODPA-BIS P and 6FDA-ODA. The scheme of preparation of the PAA based on 6FDA and ODA terminated by APTES is used as an example and it is shown in Fig. 6.

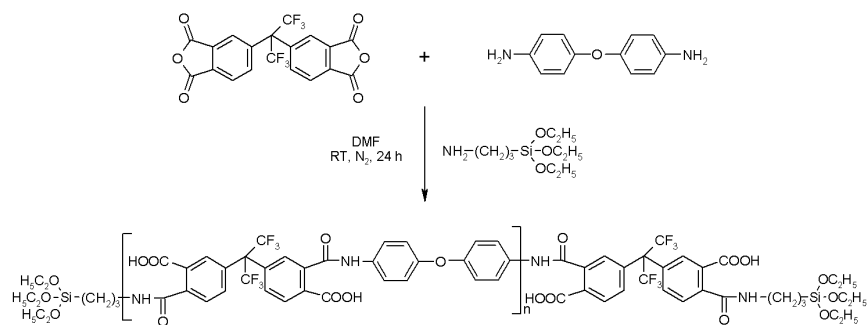


Fig. 6. Preparation of PAA (6FDA-ODA) with controlled M_n terminated by APTES.

Membranes

Mixed matrix membranes were prepared by admixing silicalite-1 crystals into the solution of APTES terminated PAA. The PAA concentration in the solution was 10 wt. %. Silicalite-1 crystals were added into the solution in such amounts to reach a range from 0 to 60 wt. % in the final MMM. Films of PI or filled PI were prepared by heat transformation of PAA solution or PAA-filler dispersion cast on a Teflon support. Final films were easily removed from Teflon support and characterized. The reaction scheme of the transformation of PAA to PI is shown in Fig. 7.

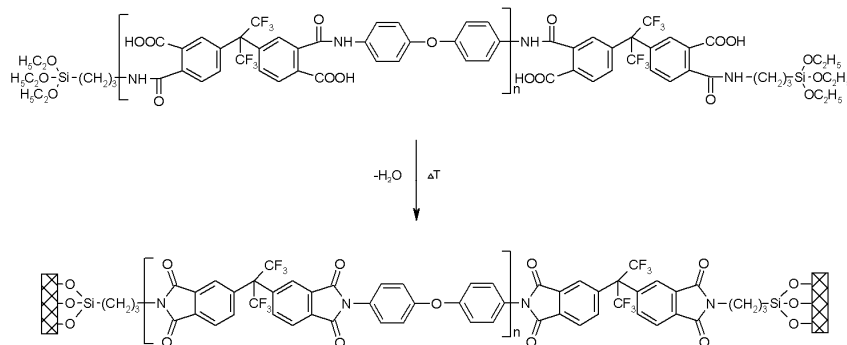


Fig. 7. Transformation of PAA (6FDA-ODA) terminated by APTES to final PI including bonding of APTES terminated polymer to silicalite-1 surface.

The polyimide type, silicalite-1 crystal size and its content in MMM are listed in Table 1.

The thickness of PI membranes was found to be in the range from 45 to 180 μm . The thickness of filled membranes increased with increasing amount of the filler.

Table 1: List of mixed matrix membranes made of APTES terminated PAA and silicalite-1 crystals.

Polyimide matrix type	Crystal size (μm)	Content of filler (wt.%)
6FDA-ODA	20, 100	0, 10, 20, 30, 40, 50, 60
PMDA-ODA	20	0, 10, 20, 30, 50
ODPA-ODA	20, 100	0, 10, 20, 30, 40, 50, 60
PMDA-BIS P	20	0, 10, 20, 30, 40
ODPA-BIS P	20	0, 10, 20, 30, 50

Permeation characteristics of the synthesized membranes

Five various types of modified PIs were used to prepare five series of membranes with different content of silicalite-1 with crystal length 20 μm and two series filled with crystals of the length 100 μm . The first set of the five series of membranes was used to study the dependence of membrane permeability on the type of polymer matrix and the amount of the filler. The content of the filler in each series ranged from 0 to 50 wt. %. The results of the permeation measurements are summarized in Fig. 8. The corresponding permeability values of the membranes for He are given together with membrane composition in Table 2. Membranes based on PI type PMDA-BIS P were rather fragile and thus, their permeabilities could not be measured.

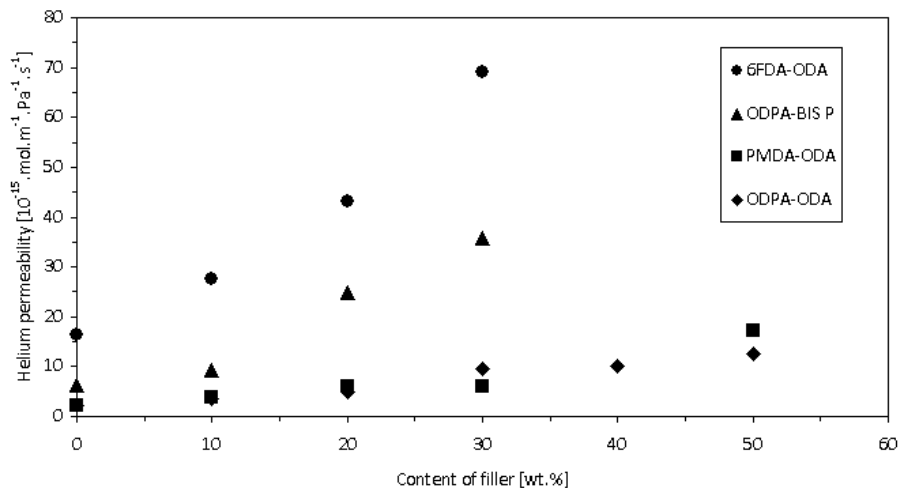
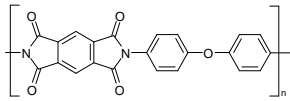
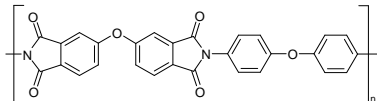
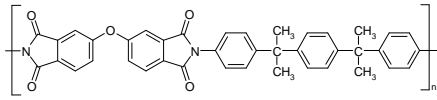
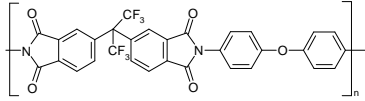


Fig. 8. Dependence of permeability of membranes filled by silicalite-1 (crystal size 20 μm) on the filler content (specification of the samples is given in Table 2).

Table 2: Permeabilities of membranes filled by silicalite-1 with crystals length 20 μm .

Polymer matrix type	Content of filler (wt.%)	Permeability of He ($10^{-15} \cdot \text{mol} \cdot \text{m}^{-1} \cdot \text{s}^{-1} \cdot \text{Pa}^{-1}$)
 PMDA-ODA	0	2.1
	10	3.7
	20	5.9
	30	6.1
	50	17.2
 ODPA-ODA	0	2.2
	10	3.5
	20	5.0
	30	9.7
	40	10.1
 ODPA-BIS P	0	6.4
	10	9.3
	20	24.7
	30	35.8
	 6FDA-ODA	0
10		27.6
20		43.2
30		69.1

One can see in Fig. 8 a pronounced dependence of the permeability on the amount of the filler in each series of these MMMs. Thus, e.g. for filler content 30 wt. % the permeability is higher as compared with that of the corresponding pure polymeric matrix by a factor ranging from 2.9 to 5.6.

The permeability depends on the type of PI matrix. It can be seen from comparison of permeability data for pure polymer matrices in Table 2. It is obvious (cf. Fig. 8) that series PMDA-ODA and ODPA-ODA have much lower permeabilities than series ODPA-BIS P and 6FDA-ODA. One can also conclude that a replacement of PMDA by ODPA in PMDA-ODA has not caused any change in the membrane permeabilities for helium. At given content of the filler are the permeabilities of the membranes based on PMDA and ODA and on ODPA and ODA practically the same for each couple. On the other hand the replacement of PMDA by 6FDA in the PMDA-ODA enhances permeabilities in comparison with the corresponding PI membranes free of filler by about factor eight i.e. from 2.1×10^{-15} to $16.3 \times 10^{-15} \text{ mol} \cdot \text{m}^{-1} \cdot \text{s}^{-1} \cdot \text{Pa}^{-1}$. This permeability increase is even more pronounced for higher content of filler in these 6FDA-ODA type membranes. Thus, e.g. permeability of membranes containing 30 wt.% of silicalite-1 was increased by more than order of magnitude from 6.1×10^{-15} to $69.1 \times 10^{-15} \text{ mol} \cdot \text{m}^{-1} \cdot \text{s}^{-1} \cdot \text{Pa}^{-1}$.

The relationship between gas permeability and d-spacing (approximate average intersegmental distances of polymers) was referred to by many authors, e.g. by Kesting [8]. The value of d-spacing is 0.46 nm for PMDA-ODA and 0.56 nm for 6FDA-ODA.

10

The ODA segment is the dominant factor in the determination of the d-spacing and the intrasegmental motions which are involved in translational mobility of dissolved molecules. Replacement of PMDA with 6FDA causes a significant increase in d-spacing. At the same time the number of mobile -O- linkages is decreased by about 40 % per unit volume in the 6FDA-ODA and mobility is further restricted by the $-C(CF_3)_2-$ linkages [8]. Thus the increase in free volume and chain stiffness work in concert to increase penetrant permeability.

An equivalent explanation can be applied to the increase of permeability after the replacement of ODA by BIS P in ODP-ODA. The effect of this replacement is less pronounced than the one found after replacement of PMDA by 6FDA. The reason most likely is a smaller size difference between linkages $-C(CH_3)_2-$ and -O- than that between $-C(CF_3)_2-$ and -O-.

Furthermore, it can be seen that MMMs permeabilities significantly depend on the filler content. They increase monotonously with increasing filler content. A more detailed analysis of the shape of the dependences is given below.

The permeabilities of some membranes containing 50 and 60 wt. % of the filler are not shown in Fig. 8. This is because during the permeability measurement they behaved as the defective membranes.

Slightly different behaviour was found for membrane series based on 6FDA-ODA filled with silicalite-1 crystal size 100 μm as it is shown in Fig. 9. There is a remarkably steep increase in membrane permeabilities for higher filler content. Thus the permeability value for membrane based on 6FDA-ODA with filler content of 50 wt. % is about 10 times higher than that of the corresponding pure PI membrane. The explanation could be sought in filler distribution in membranes containing more than 30 wt. % of filler. As an example the structure of membrane based on 6FDA-ODA and 60 wt.% of filler revealed by SEM is shown in Fig. 10.

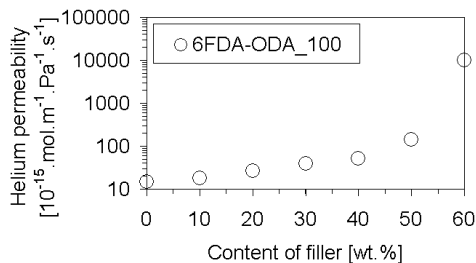


Fig. 9: Dependence of permeability of membranes filled by silicalite-1 (crystal size 100 μm) on the filler content

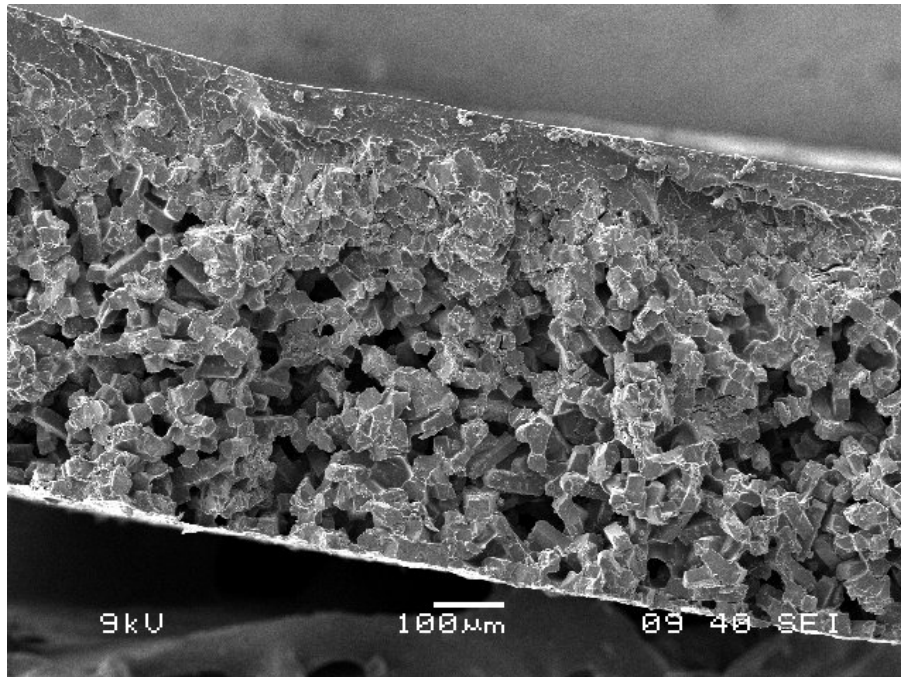


Fig. 10. The SEM image of membrane made of PI(6FDA-ODA) filled by 60 wt. % of silicalite-1.

It appears (cf. Fig. 10) that the membrane is stratified. In particular, more than 4/5 of the membrane depth represents a layer containing macropores and only a layer of the thickness of about 100 μm represents a compact mixed matrix composite. The thickness of this composite layer is comparable with the silicalite-1 crystals length (100 μm). In this way paths of very low mass transport resistances were formed.

A similar effect of the permeability enhancement was described by Duval et al. [9] as a result of poor adhesion between rigid organic polymers and inorganic fillers. The membranes in our work were made of PI modified by APTES which is supposed to react with hydroxyl groups present on surface of silicalite-1 and thus form chemical bonds between the modified PI matrix and surface of the filler. It means that the surface of all the crystals is assumed to be covered by a PI layer. Fig. 11 showing the membrane cut with seven times higher magnification (i.e. 350×) confirms this assumption.

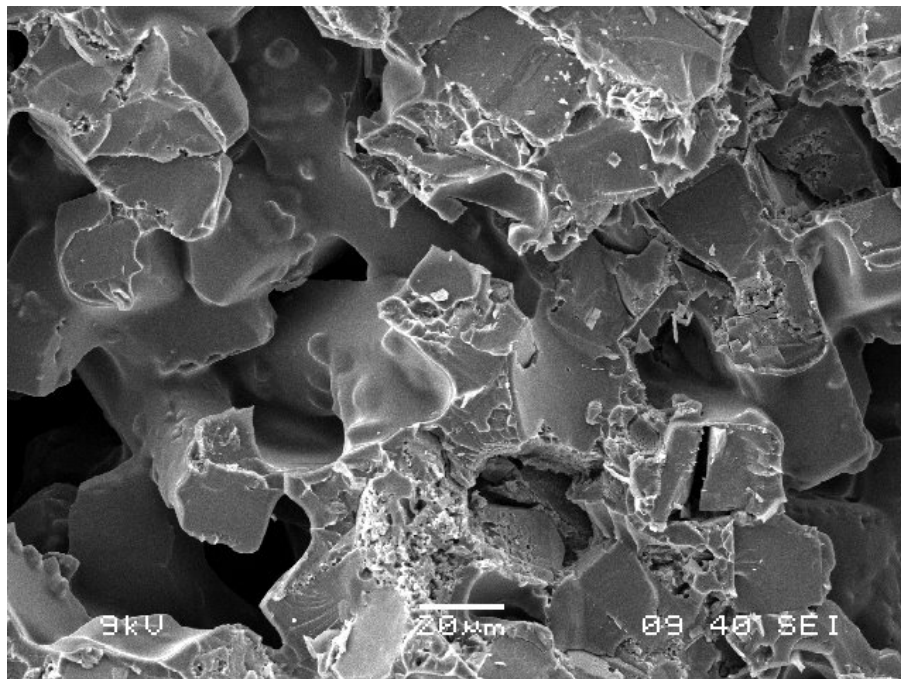


Fig. 11. The detail SEM image of membrane made of PI(6FDA-ODA) filled by 60 wt. % of silicalite-1.

Similar stratification of membranes was evidenced by for other membrane series prepared in our lab. The stratification occurred when filler content was of 50 % by mass. A formation of a layer containing macropores occurred irrespective of the accessibility the filler micropores. It appears therefore that the selected combination of PI matrices with the silicalite-1 filler or SiO₂ particles of other type might represent a novel route to preparation of asymmetric mixed matrix membranes. Such a lamellar system might contain (i) a relatively thin top layer of pure polymer, (ii) a bottom layer with a continuous system of macropores between agglutinated particles of the filler and/or (iii) a rather compact composite layer polymer + filler (free of a continuous system of macropores). We also did not observe any formation of a macroporous layer upon substitution of PI matrix modified by the APTES for polyimide-polysiloxane matrices free of any coupling agent.

Comparison of experimentally estimated permeability with a theoretical model

To compare the dependence of permeability on the content of the filler the theoretical Bruggeman model (5) was applied.

$$\left[\frac{(P_{eff}/P_c) - (P_d/P_c)}{1 - (P_d/P_c)} \right] \left(\frac{P_{eff}}{P_c} \right)^{-1/3} = 1 - \phi_d \quad (5)$$

13

where P_{eff} is the effective permeability of the membrane, P_c and P_d are permeabilities of continuous and dispersed phase, respectively, and ϕ_d is the volume fraction of the dispersed phase (filler) in the membrane.

The relation between the mass fraction of dispersed phase w_d and the corresponding volume fraction of dispersed phase ϕ_d is given by Eq (6).

$$\phi_d = \frac{w_d \left(\frac{\rho_c}{\rho_d} \right)}{1 - w_d \left(1 - \frac{\rho_c}{\rho_d} \right)} \quad (6)$$

Here ρ_c and ρ_d are densities of the continuous and dispersed phases, respectively. When the continuous phase is PI (6FDA-ODA) and the dispersed phase calcined silicalite-1 then $\rho_c = 1.43 \text{ g.cm}^{-3}$ [8] and $\rho_d = 1.78 \text{ g.cm}^{-3}$ [10]. The values of volume fraction together with the corresponding mass fraction are given in Table 3.

Table 3: Values of volume fraction, ϕ_d , together with the corresponding mass fraction w_d

w_d	0	10	20	30	40	50
ϕ_d	0	8	17	26	35	45

When silicalite-1 crystals form the dispersed phases, its permeability can be expressed as:

$$P_d = D_{intra} \frac{\beta_{intra}}{RT} \quad (7)$$

where D_{intra} is the intracrystalline diffusivity of the penetrant in the silicalite-1 crystals, β_{intra} the intracrystalline porosity, R the gas constant and T the temperature. We took as an estimate of the intracrystalline diffusivity of helium the value $D_{intra} = 7.65 \times 10^{-8} \text{ m}^2 \cdot \text{s}^{-1}$ based on molecular simulation [11], $\beta_{intra} = 0.35$ and the temperature T of measurement was $T = 298 \text{ K}$; then $P_d = 1.08 \times 10^{-11} \text{ mol.m}^{-1} \cdot \text{s}^{-1} \cdot \text{Pa}^{-1}$.

As shown in Table 2 the permeabilities of continuous phases P_c for helium were found for prepared membranes to be between 2.1×10^{-15} and $16.3 \times 10^{-15} \text{ mol.m}^{-1} \cdot \text{s}^{-1} \cdot \text{Pa}^{-1}$. This estimate shows that the permeability of the dispersed phase is much larger than that one of continuous phase, i.e. $P_d \gg P_c$. The other limiting case is that one for impermeable particles of dispersed phase i.e. for $P_c \gg P_d$. Then the Bruggeman model can be simplified for the composite materials in this work with $P_d / P_c \gg 1$ and $P_{eff} / P_c \ll P_d / P_c$ to Eq (8).

$$\frac{P_{eff}}{P_c} = \frac{1}{(1 - \phi_d)^3} \quad (8)$$

The limiting case for impermeable particles of dispersed phase is represented by the conditions $P_d / P_c \ll 1$ and $P_{eff} / P_c \gg P_d / P_c$ and the expression for P_{eff} / P_c reduces to Eq (9).

$$\frac{P_{eff}}{P_c} = (1 - \phi_d)^{3/2} \quad (9)$$

It can be seen from Eqs (8), (9) that for limiting situations the dimensionless parameter P_{eff} / P_c is a function of a single parameter ϕ_d and it does not depend any more on the permeability of dispersed phase.

The values of the parameter P_{eff} / P_c together with volume fractions of crystals for membranes prepared from polyimides modified by the coupling agent are given in Table 4. Theoretical values of the dimensionless parameter P_{eff} / P_c together with volume fractions of crystals are given in Table 5. The values of the parameter P_{eff} / P_c were obtained from experiment and corresponding theoretical data were calculated according to Eq (8) derived from Bruggeman model. The dependences of the parameter P_{eff} / P_c on the content of the filler are shown in Fig. 13 and Fig. 12.

Table 4: Experimental values of the dimensionless parameter P_{eff} / P_c

ϕ_d	P_{eff} / P_c				
	PMDA-ODA	ODPA-ODA	ODPA-BIS P	6FDA-ODA	6FDA-DA_100
0	1.00	1.00	1.00	1.00	1.00
0.08	1.75	1.56	1.46	1.70	1.23
0.17	2.78	2.21	3.87	2.66	1.84
0.26	2.84	4.29	5.62	4.24	2.68
0.35	-	4.49	-	-	3.58
0.45	8.06	-	-	-	9.69

Table 5: Theoretical values of the dimensionless parameter P_{eff} / P_c

ϕ_d	0	0.08	0.17	0.26	0.35	0.45
P_{eff} / P_c	1.00	1.29	1.73	2.43	3.62	5.86

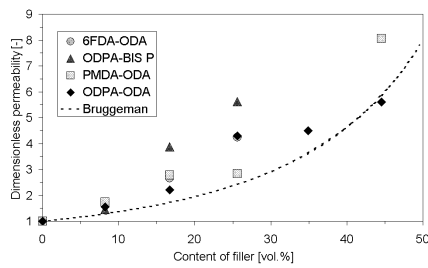


Fig. 13: The comparison of experimental and theoretical dependences of the dimensionless permeability on the filler content for membrane series containing silicalite-1 crystals of size 20 μm .

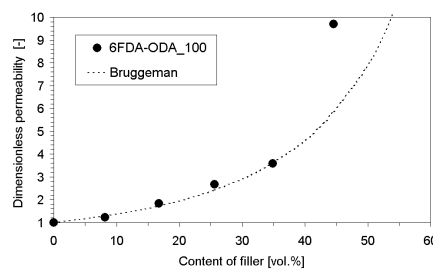


Fig. 12: The comparison of experimental and theoretical dependences of the dimensionless permeability on filler content for membrane series containing silicalite-1 crystals of size 100 μm .

It appears that practically in all the cases the experimental curves get ahead of the theoretical ones. It should be noted that the theoretical model considered is valid for a quasihomogeneous distribution of the filler particles in the membrane. At the same time

15

the Bruggeman model refers to stochastic distributions (random dispersion) of the dispersed phase. A plausible explanation of the permeation data deviation from the above theoretical model appears to be the stratification of the mixed matrix membranes. In the simplest case when the stratified membrane is formed by a two layer laminate with one layer containing a continuous system of macropores and the other one represented by dense polymer free of filler this conclusion is obvious due to a negligible mass transport resistance of the macropores.

4. Conclusion

A novel preparation approach was used in this study to improve interfacial adhesion of membrane constituents. It consisted in the use of coupling agent 3-aminopropyltriethoxysilane. Polyimide chains were thus first endcapped by the coupling agent and subsequently this modification enabled their reaction with silicalite-1 terminal OH groups at outer crystal surface of silicalite-1.

The principal membrane characteristic evaluated was the plot of relative membrane permeability P_{eff}/P_c vs. ϕ_d where P_{eff} and P_c [$\text{mol}\cdot\text{m}^{-1}\cdot\text{s}^{-1}\cdot\text{Pa}^{-1}$] denote the effective permeability of mixed matrix membrane and that of continuous phase, respectively and ϕ_d stands for volumetric fraction of dispersed phase (silicalite-1). The other membrane characterization was carried out by SEM. The accessibility of silicalite-1 channel system for molecules of penetrants after crystal embedding into polymer was examined by iodine indicator technique.

The experimental P_{eff}/P_c vs. ϕ_d plots were compared with theoretical dependences simulated using the Bruggeman model. It should be noted that P_{eff}/P_c vs. ϕ_d plots were always monotonous but experimental data exhibited significant deviation from the Bruggeman model. The analysis showed that the above deviation can be explained by stratification of the composite membrane which can be considered as consisting of two or even three layers as evidenced by SEM micrographs.

Acknowledgement The financial support by the Czech Science Foundation via grant No. 203/09/1353 is gratefully acknowledged.

References

- [1] T. S. Chung, L. Y. Jiang, Y. Li, S. Kulprathipanja, *Prog. Polym. Sci.* 32 (2007) 483–507.
- [2] J. Kornatowski, *Zeolites*, 8 (1988) 77-78.
- [3] M.S. Frycova, M. Kocirik, A. Zikanova, P. Sysel, B. Bernauer, V. Krystl, I. Huttel, J. Hradil, M. Eic, *Adsorpt. Sci. Technol.*, 23 (2005) 595-605.
- [4] H. Haken, H.C. Wolf, *Molecular Physics and Elements of Quantum Chemistry*. Springer, Berlin, 2004.
- [5] A. Bondi, Van der Waals Volumes and Radii. *J. Phys. Chem.*, 68 (1964) 441-451.
- [6] M. Kocirik, J. Kornatowski, V. Masarik, P. Novak, A. Zikanova, J. Maixner, *Microporous Mesoporous Mater.* 23 (1998) 295-308.
- [7] M. Frycova, *Mixed matrix membranes based on modified polyimides and inorganic fillers*, Ph.D. Thesis, ICT Prague, Prague, 2008.

16

- [8] R.E. Kesting, A.K. Fritzsche. *Polymeric Gas Separation Membranes*, Wiley Interscience, New York, 1993.
- [9] J.-M. Duval, A.J.B. Kemperman, B. Folkers, M.H.V. Mulder, G. Desgrandchamps, C.A. Smolders, *J. Appl. Polym. Sci.* 54 (1994) 409-418.
- [10] E.M. Flanigen, J.M. Bennett, R.W. Grose, J.P. Cohen, R.L. Patton, R.M. Kirchner, J.V. Smith, *Nature*, 271 (1978) 512-516.
- [11] R. Nagumo, H. Takaba, S. Suzuki, S. Nakao, *Microporous Mesoporous Mater.*, 48 (2001) 247-254.